Tensely strained GeSn alloys as optical gain media

S. Wirths, Z. Ikonic, A. T. Tiedemann, B. Holländer, T. Stoica, G. Mussler, U. Breuer, J. M. Hartmann, A. Benedetti, S. Chiussi, D. Grützmacher, S. Mantl, and D. Buca

Citation: Applied Physics Letters **103**, 192110 (2013); doi: 10.1063/1.4829360
View online: http://dx.doi.org/10.1063/1.4829360
View Table of Contents: http://scitation.aip.org/content/aip/journal/apl/103/19?ver=pdfcov
Published by the AIP Publishing

Tensely strained GeSn alloys as optical gain media

S. Wirths,[1,a)] Z. Ikonic,[2] A. T. Tiedemann,[1] B. Holländer,[1] T. Stoica,[1] G. Mussler,[1] U. Breuer,[3] J. M. Hartmann,[4] A. Benedetti,[5] S. Chiussi,[5] D. Grützmacher,[1] S. Mantl,[1] and D. Buca[1]

[1]*Peter Grünberg Institute 9 (PGI 9) and JARA-Fundamentals of Future Information Technologies, Forschungszentrum Juelich, 52425 Juelich, Germany*
[2]*Institute of Microwaves and Photonics, School of Electronic and Electrical Engineering, University of Leeds, Leeds LS2 9JT, United Kingdom*
[3]*Central Institute for Engineering, Electronics and Analytics (ZEA-3), Forschungszentrum Juelich, 52425 Juelich, Germany*
[4]*CEA, LETI, Minatec Campus, 17 rue des Martyrs, 38054 Grenoble, France*
[5]*Dpto. Física Aplicada and CACTI, Univ. de Vigo, Campus Universitario Vigo, 36310 Vigo, Spain*

(Received 6 September 2013; accepted 22 October 2013; published online 7 November 2013)

This letter presents the epitaxial growth and characterization of a heterostructure for an electrically injected laser, based on a strained GeSn active well. The elastic strain within the GeSn well can be tuned from compressive to tensile by high quality large Sn content (Si)GeSn buffers. The optimum combination of tensile strain and Sn alloying softens the requirements upon indirect to direct bandgap transition. We theoretically discuss the strain-doping relation for maximum net gain in the GeSn active layer. Employing tensile strain of 0.5% enables reasonable high optical gain values for $Ge_{0.94}Sn_{0.06}$ and even without any n-type doping for $Ge_{0.92}Sn_{0.08}$. © *2013 AIP Publishing LLC*. [http://dx.doi.org/10.1063/1.4829360]

Silicon and Germanium group IV semiconductors have been implemented into photonic devices, but so far mainly as passive optoelectronic components.[1–3] The indirect bandgap of these semiconductors makes the realization of active components such as Light Emitting Diodes or lasers, challenging.[4] A silicon-based optically pumped laser was reported in 2005, with a nano-patterned silicon film, where the light emission originated from defects in the etched side walls of the film.[5] A Si Raman laser was demonstrated by Boyraz and Jalali[6] and, very recently, Camacho *et al.*[7] made use of heavily n-doped Ge under 0.2% tensile strain to demonstrate an electrically pumped laser. The threshold current density, however, is prohibitively large for practical applications. Therefore, considerable effort has to be directed towards increasing the light emission efficiency of group IV semiconductors. For this purpose either alloying Ge with Sn or introducing sufficient tensile strain has been proposed, since both Sn and strain are expected to reduce the direct bandgap of Ge faster than its indirect band-gap.[8,9] Both approaches are supported by the recent achievements in synthesizing high quality GeSn alloys[10] and the demonstration of uniaxially tensile strained Ge nanowires (NW) to a record value of 3%.[11]

This letter presents the growth of GeSn layers with strain varying from compressive to tensile, which will serve as active layer in an electrically pumped laser. This is realized using high quality (Si)GeSn buffers which may be used later on as cladding layers for a quantum well layer structure. Second, with emphasis on the experimentally realized structures, we discuss, based on net gain calculations, the optimum conditions regarding strain, Sn content, and n-doping in order to maximize laser gain. The role of the tensile strain on the evolution of gain is also highlighted.

[a)]Author to whom correspondence should be addressed. Electronic mail: s.wirths@fz-juelich.de

The growth of (Si)GeSn was reported earlier by Bauer *et al.* in an ultra-high vacuum—chemical vapour deposition tool.[12] However, high quality GeSn layers were only recently achieved in production tools.[10,13,14] Our growth studies were performed in an industry-compatible Reduced Pressure Chemical Vapor Deposition (RP-CVD) AIXTRON TRICENT® reactor with a showerhead which provides a highly uniform gas precursor distribution over 200 mm wafers.[15–17] (Si)GeSn layers were grown on Ge virtual substrates (VS)[18] on p-type ($<1 \times 10^{15}$ cm^{-3}) 200 mm Si(100) wafers using Si_2H_6, Ge_2H_6 gas (10% diluted in H_2) and $SnCl_4$.[14] Structural data associated with compressively strained and partially relaxed GeSn layers (degree of relaxation R = 58%) with Sn contents up to 13.5% grown on Ge VS are provided in Fig. 1. X-ray diffraction (XRD) θ–2θ scans around the (004) reflection (Fig. 1(a)) indicate pseudomorphic GeSn layers. The presence of well-defined Pendellösung fringes around the GeSn peaks evidences the high crystalline quality of the layers with smooth surfaces and abrupt interfaces. Moreover, the GeSn peak shifts towards lower angles for higher Sn concentrations indicating larger out-of-plane lattice constants and hence larger compressive in-plane strain.

Layers grown above the critical thickness for strain relaxation will plastically relax to a larger in-plane lattice constant. They are appropriate as buffers (later also claddings) to compressively or tensely strain thin GeSn layers with higher or lower Sn content, respectively, grown on top (active layers). We show for instance in Fig. 1(b) Reciprocal Space Maps (RSM) around the (224) asymmetric order for partially relaxed 250 nm thick $Ge_{0.865}Sn_{0.135}$ (R = 58%) and 300 nm thick $Si_{0.04}Ge_{0.82}Sn_{0.14}$ (R = 60%) layers grown on Ge VS. The RSM allows the determination of the lattice constants of the tetragonal structures which are in both cases approximately $a_{par} = 5.73$ Å and $a_{per} = 5.8$ Å for the in-plane

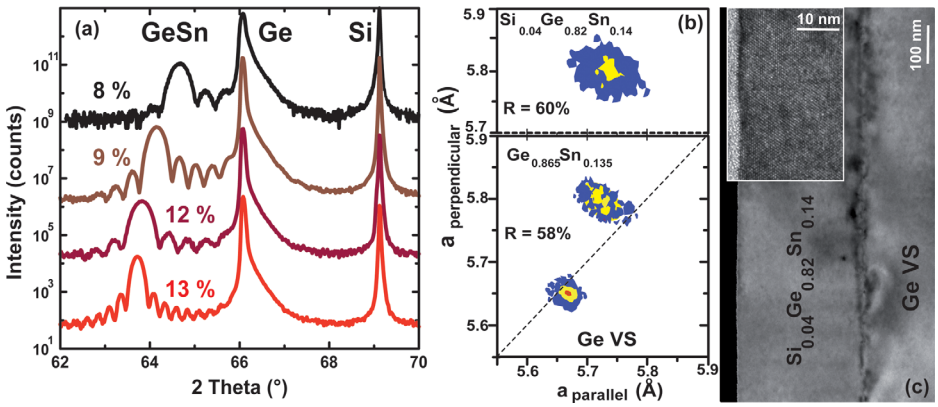

FIG. 1. (a) XRD θ–2θ scans around the (004) order associated to pseudomorphic GeSn layers grown on Ge VS with Sn contents from 8% to 13%. (b) RSM around the (224) asymmetric reflection for 250 nm $Ge_{0.865}Sn_{0.135}$ and 300 nm $Si_{0.04}Ge_{0.82}Sn_{0.14}$ layers grown on Ge VS. The in- and out-of-plane lattice constants of the (Si)GeSn crystals were extracted to evaluate the degree of strain relaxation. (c) XTEM images of partially strain relaxed $Si_{0.04}Ge_{0.82}Sn_{0.14}$ layers used later on as buffers for strained GeSn layers.

and out-of-plane lattice constants, respectively. The formation of a misfit dislocation (MD) network at the (Si)GeSn/Ge VS interface, as seen in the cross section transmission electron microscope (XTEM) micrograph in Fig. 1(c) for 60% relaxed 300 nm $Si_{0.04}Ge_{0.82}Sn_{0.14}$, evidences lattice relaxation. Similar to the growth of low temperature Ge buffers,[19] but different from relaxed SiGe buffers, no threading dislocations crossing the relaxed GeSn layer were observed for all investigated structures. The above results demonstrate the possibility of tuning the lattice constants and, hence, the elastic strain, especially tensile strain as shown below, in Ge(Sn) layers grown on top of these high Sn content (Si)GeSn buffers. The use of partially relaxed GeSn buffers to strain epitaxial Ge up to 1.3% has been recently achieved.[14] We point out the use of SiGeSn as buffer layers while SiGeSn are also more suitable as laser claddings due to the indirect gap and the lower absorption compared to GeSn layers.[20]

The bandgaps and band offsets of strained and relaxed binary GeSn alloys, as well as of the ternary SiGeSn layers, have been calculated from the supercell empirical pseudopotential method,[8,14] together with linear interpolation of deformation potentials[21] and band offsets[22] of elemental Si, Ge, and Sn. The calculated conduction and valence bands indicate that all $GeSn_x$ layers with $x < 10\%$, including pure Ge ($x = 0$), grown directly on a fully relaxed (cubic) or on partially relaxed (tetragonal) $Ge_{1-y}Sn_y$ ($x < y \geq 12$) are direct bandgap semiconductors. For laser structure we propose to use indirect gap (Si)GeSn buffer and claddings and a strained GeSn active well. The growth of such heterostructures requires (i) a certain thickness of the buffer to induce sufficient strain relaxation and (ii) a total structure thickness to prevent epitaxial breakdown due to Sn precipitation. The coherent growth of a B doped 40 nm $Si_{0.12}Ge_{0.84}Sn_{0.04}$ layer (later hole injection layer) followed by a 35 nm $Ge_{0.93}Sn_{0.07}$ (later active layer) is shown in Fig. 2(a). The pseudomorphic nature of interfaces without Sn segregation and the high quality of the heterostructure are demonstrated by the XTEM and High resolution (HR) TEM micrographs. The steep slope of the Sn, Si, and B signals in the superimposed Secondary Ions Mass Spectrometry (SIMS) depth profiles are characteristics of abrupt interfaces. The $Ge_{0.93}Sn_{0.07}$ layer grown on top of the $Si_{0.12}Ge_{0.84}Sn_{0.04}$ buffer with a Ge VS lattice constant is *compressively* strained. For the laser active wells intended here, buffers able to induce *tensile* biaxial strain are aimed. Therefore, a stack consisting of 25 nm $Ge_{0.92}Sn_{0.08}$/295 nm $Ge_{0.88}Sn_{0.12}$/Ge VS has been grown, as presented in Fig. 2(b). Note that in order to separate the Sn signals originating from the two GeSn layers, a 10 nm Ge spacer is used. Thus, the crystalline quality and the strain status of the topmost GeSn layer can be investigated in detail. The high quality of the stack is shown by the very low Rutherford Backscattering Spectrometry (RBS) channeling minimum yield of 6% in the Sn signal of the top $Ge_{0.92}Sn_{0.08}$ layer. This is a direct experimental proof of a low defect density in the thick, partially relaxed GeSn buffer layer.

Quantitative determination of strain in thin strained $Ge_{1-x}Sn_x/Ge_{1-y}Sn_y$ ($x < y$) heterostructures is a challenging task. Ion channeling angular yield scans provide absolute angles between various crystal directions and allow the deduction of the full strain tensor.[23] We performed ion channeling angular scans of the Sn backscattering signal through the [001] sample normal and the [011] direction in the (100) plane. The position of the scan minimum represents the absolute angle $\theta_{[011]}$ between the [001] sample normal and the inclined [011] direction, amounting to 45° for cubic lattices. Compressive/tensile tetragonal strain in GeSn leads to a

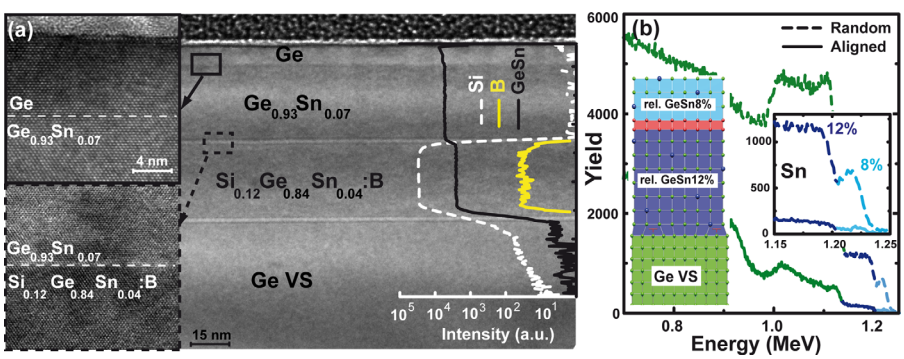

FIG. 2. (a) XTEM image of 8 nm Ge/35 nm $Ge_{0.93}Sn_{0.07}$/40 nm $Si_{0.12}Ge_{0.84}Sn_{0.04}$:B/Ge VS heterostructure. The HR-TEM insets demonstrate the pseudomorphic interfaces while the SIMS spectra prove the sharp Sn and B elements interface distributions. (b) RBS random and aligned spectra of 25 nm $Ge_{0.92}Sn_{0.08}$/295 nm $Ge_{0.88}Sn_{0.12}$/Ge VS.

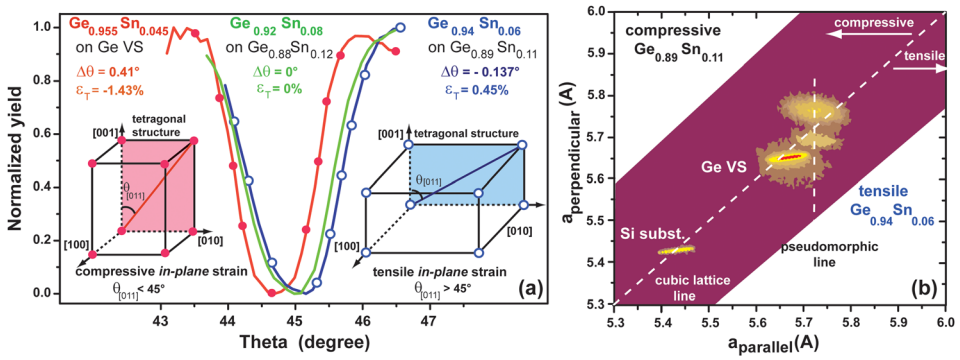

FIG. 3. Angular channeling scans in the [011] direction of (full red circles) 30 nm $Ge_{0.955}Sn_{0.045}$/200 nm thin compressive Ge, (green line) 25 nm $Ge_{0.92}Sn_{0.08}$/295 nm $Ge_{0.88}Sn_{0.12}$/Ge VS and (empty blue circles) 30 nm $Ge_{0.94}Sn_{0.6}$ /265 nm $Ge_{0.89}Sn_{0.11}$/Ge VS. The angular deviation from the cubic lattice and the calculated tetragonal strain are given. (b) RSM of 30 nm $Ge_{0.94}Sn_{0.06}$/265 nm$Ge_{0.89}Sn_{0.11}$/Ge VS layer indicating pseudomorphic growth of the topmost $Ge_{0.94}Sn_{0.06}$ layer.

smaller/larger angle ($45° - \Delta\theta_{[011]}$), respectively. For symmetric (isotropic) biaxial strain, the amount of tetragonal strain is related to the angular shift as $\varepsilon_T = -2 \cdot \Delta\theta_{[011]}$.

The ion channeling angular yield measurements for three different heterostructures with a top GeSn layer under either compressive strain, strain-relaxed and tensile strain conditions are presented in Fig. 3. Based on Vegard's Law, the angular displacement associated to a pseudomorphic GeSn layer with 4.5 at. % Sn on cubic Ge should be $\Delta\theta_{[011]}^{GeSn,th} = 0.30°$. Taking into account the $\Delta\theta_{[011]}^{Ge} = 0.11°$ of the slightly compressively strained Ge buffer used for that specific case, the angular deviation of $\Delta\theta_{[011]}^{GeSn} = 0.41°$ from the cubic crystal lattice confirms the pseudomorphic growth of $Ge_{0.955}Sn_{0.045}$ on the Ge thin buffer. The corresponding compressive tetragonal strain is then −1.43%.

In agreement with theory, a fully strain relaxed (cubic) $Ge_{0.92}Sn_{0.08}$ layer was obtained by epitaxial growth on a 73% strain relaxed $Ge_{0.88}Sn_{0.12}$ buffer (no deviation from 45° in Fig. 3(a)). This cubic structure alloy has been shown to be a direct gap semiconductor.[24,25] Finally, the angular channeling scan for a *tensely* strained 30 nm $Ge_{0.94}Sn_{0.06}$ grown on partially relaxed (R = 69%) 265 nm $Ge_{0.89}Sn_{0.11}$ buffer is shown. The angular deviation of $\Delta\theta^{GeSn} = -0.137°$ translates into a tetragonal strain of 0.45%. The results of channeling experiments are confirmed by RSM presented in Fig. 3(b). Besides the Si substrate and the Ge VS peaks, two well-defined GeSn peaks on both sides of the cubic lattice line are resolved, which originate from the slightly compressively strained $Ge_{0.89}Sn_{0.11}$ buffer and the tensile strained $Ge_{0.94}Sn_{0.06}$ layer. The identical in-plane lattice constant of these GeSn layers evidences pseudomorphic growth.

We next investigate the potential of these strained layers for optoelectronic applications by calculating optical gain. Previously, calculations have been presented for a GeSn/SiGeSn multiple quantum wells laser,[21,26–28] but only relaxed or compressively strained layers were considered. The impact of tensile strain on the optical gain in pure Ge was only very recently investigated.[29] Here we calculate the optical gain including also the intra-valence band (IVB) absorption, not considered in previous calculation for Ge(Sn) based system.

The gain calculation was performed using the 8 × 8 k·p model, with strain effects included.[30,31] Since the layers of interest are relatively thick, tens of nm, size-quantization effects will not be prominent, and thus bulk properties were considered. The material parameters were taken as listed in Ref. 21, except for the Luttinger-Kane parameters. Their calculation in alloys, using the empirical pseudopotential method[32] showed non-linear dependence on Sn content, very different from the linear interpolation used in Ref. 21 We have, therefore, employed quadratic interpolation of the data set in Ref. 32 The carrier distribution within each band is considered to be in equilibrium at 300 K. By including transitions between all bands within the 8 × 8 k·p model, the calculated gain accounts for: (i) the interband (IB) valence-conduction band transitions, which may provide gain or absorption and (ii) IVB transitions[33,34] between heavy-hole (HH)/light-hole (LH) and split-off hole bands due to spin orbit coupling (SO) bands, which bring in additional absorption. Free-carrier (scattering induced) absorption is not included in these calculations, thus the presented data correspond to the upper limit of the gain achievable in these systems.

The carrier density contour lines with a practically significant peak net gain of 500 cm^{-1} for the $Ge_{0.94}Sn_{0.06}$ and $Ge_{0.92}Sn_{0.08}$ layers under relaxed and 0.5% tensile strain conditions, discussed above, are shown in Fig. 4. Clearly, the electron density has to be larger than, or equal to, the hole density (the difference of the two is the effective n-type doping density, and the hole density is the injected carrier density). The full contour plot with the 500, 3000, and 5000 cm^{-1} contour lines is shown in the inset for 0.4% tensile strained $Ge_{0.94}Sn_{0.06}$.

From Fig. 4 one can see that for the (indirect band gap) $Ge_{0.94}Sn_{0.06}$ alloy a significant n-doping in its relaxed state is required in order to achieve any meaningful gain, but quite a

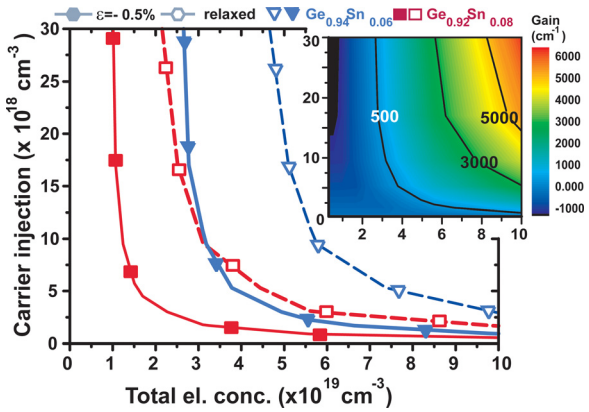

FIG. 4. The 500 cm^{-1} contour line plot of the gain for $Ge_{0.94}Sn_{0.06}$ and $Ge_{0.92}Sn_{0.08}$ materials for the relaxed and 0.5% tensile strained cases. The carrier injection represents the hole density while the n-doping is given by the difference of the total electron concentration and the injected carrier density. The contour plot for 0.4% tensely strained $Ge_{0.94}Sn_{0.06}$ alloy is given in the inset. The contour lines where the peak gain amounts to 500, 3000, and 5000 cm^{-1} are highlighted.

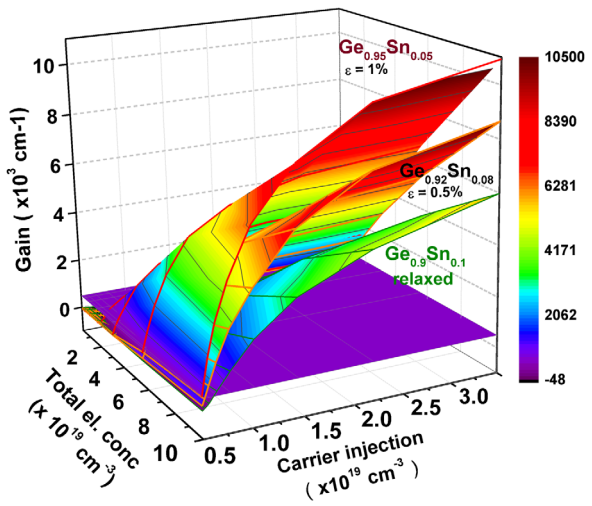

FIG. 5. Comparison of GeSn materials with direct gaps under different strain conditions: $Ge_{0.95}Sn_{0.05}$ under 1% tensile strain, $Ge_{0.82}Sn_{0.08}$ under 0.5% tensile strain and fully relaxed $Ge_{0.9}Sn_{0.1}$.

decent gain is expected for a small tensile strain, i.e., 0.4% (at injected carrier density in excess of 5×10^{18} cm^{-3}). In this alloy a large gain of 3×10^3 cm^{-1} occurs at photon energy ~648 (586) meV in relaxed (or 0.4% tensile strain) state, and the IVB absorption is not a major problem even for the largest hole densities considered (in the sense that gain only increases with hole density). This situation is similar for a relaxed $Ge_{0.92}Sn_{0.08}$ alloy (just direct according to Ref. 25). In its unstrained state, a moderately high n-doping of 3×10^{19} cm^{-3} is required to achieve gain. Similarly, for a small tensile strain of 0.5%, a gain of $>10^3$ cm^{-1} (peaking at ~488 meV) without any doping becomes possible. However, this is observed at quite large injected carrier densities of $\sim 1.7 \times 10^{19}$ cm^{-3}. Similar behavior is observed for $Ge_{0.94}Sn_{0.06}$ alloy under 1% tensile strain (Fig. 5).

An increase of the degree of relaxation of the buffer, as presented here, allows higher tensile strains, a route to obtain gain without doping. However, a significant IVB absorption then sets in, visible from the gain decreasing for too large hole densities, a feature which was almost absent in the unstrained case. As displayed in Fig. 5, higher tensile strain applied to lower Sn content alloys offers a larger gain then available in direct gap GeSn layers with larger Sn content at a lower strain (including fully strain relaxed). For $Ge_{0.92}Sn_{0.08}$ strained by 1%, the IVB induced bowing down of gain would require slightly larger hole densities for lasing than were considered here.

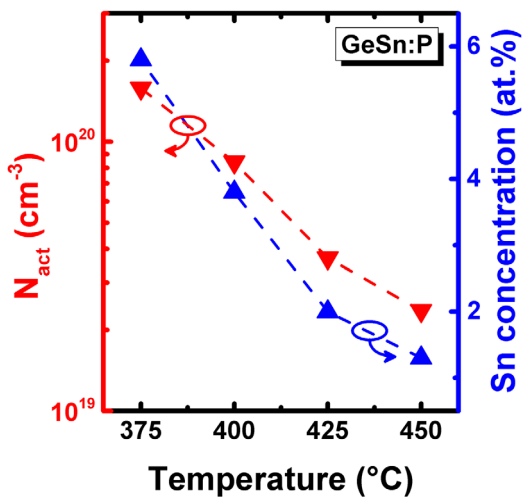

FIG. 6. Electrically active dopant concentrations in GeSn alloys as measured by ECV for constant $Ge_2H_6/SnCl_4$ flow ratio and PH_3 partial pressure versus temperature.

The gain calculation indicates that the required n-type doping is in the 5×10^{18}–5×10^{19} cm^{-3} range for the GeSn active layer. Higher active dopant concentrations are, however, needed for cladding layers for electrical injection. *In-situ* n-doping of (Si)GeSn layers was studied using PH_3/B_2H_6 precursors. The concentration of electrically active P in GeSn versus the growth temperature is plotted in Fig. 6. Maximum active P concentration of 1.5×10^{20} cm^{-3} in both GeSn:P and SiGeSn:P values close to 100% activation of dopants was determined by SIMS and electrochemical capacity voltage (ECV) measurements. The B concentration in the SiGeSn layer discussed in Fig. 2(a) amounts to 2×10^{19} cm^{-3}.

In conclusion, we have presented the growth of GeSn heterostructures for laser applications. Tensile strained $Ge_{0.95}Sn_{0.05}$ and $Ge_{0.82}Sn_{0.08}$ active layers on lattice matched SiGeSn claddings and the *in-situ* doping of these layers were investigated. The strain in the active layer can be adjusted via lattice engineered SiGeSn ternaries. The 8×8 k·p model was used to study the influence of strain on the optical gain, including the role of inter-valence band absorption. We show that the requirement for heavy n-type doping, used previously for strained Ge, can be relaxed by suitable combination of alloy composition and strain, and thus lasing without n-doping is possible. Moreover, while the tensile strain is largely beneficial for indirect GeSn layers, high strain levels may also have the drawback of inducing valence subband splitting which strongly increases the IVB absorption. The availability of these materials and theoretical considerations indicate that efficient lasing in group IV semiconductors should be demonstrated quite soon.

[1]G. T. Reed, G. Mashanovich, F. Y. Gardes, and D. J. Thomson, Nat. Photonics **4**, 518 (2010).
[2]D. Buca, S. Winnerl, S. Lenk, C. Buchal, and D.-X. Xu, Appl. Phys. Lett. **80**, 4172 (2002).
[3]D. Buca, S. Winnerl, S. Lenk, S. Mantl, and C. Buchal, J. Appl. Phys. **92**, 7599 (2002).
[4]D. Liang and J. E. Bowers, Nat. Photonics **4**, 511 (2010).
[5]S. G. Cloutier, P. A. Kossyrev, and J. Xu, Nature Mater. **4**, 887 (2005).
[6]O. Boyraz and B. Jalali, Opt. Express **13**, 796 (2005).
[7]R. E. Camacho-Aguilera, Y. Cai, N. Patel, J. T. Bessette, M. Romagnoli, L. C. Kimerling, and J. Michel, Opt. Express **20**, 11316 (2012).
[8]P. Moontragoon, P. Pengpit, T. Burinprakhon, S. Maensiri, N. Vukmirovic, Z. Ikonic, and P. Harrison, J. Non-Cryst. Solids **358**, 2096 (2012).
[9]P. Moontragoon, Z. Ikonić, and P. Harrison, Semicond. Sci. Technol. **22**, 742 (2007).
[10]B. Vincent, F. Gencarelli, H. Bender, C. Merckling, B. Douhard, D. H. Petersen, O. Hansen, H. H. Henrichsen, J. Meersschaut, W. Vandervorst, M. Heyns, R. Loo, and M. Caymax, Appl. Phys. Lett. **99**, 152103 (2011).
[11]M. J. Süess, R. Geiger, R. A. Minamisawa, G. Schiefler, J. Frigerio, D. Chrastina, G. Isella, R. Spolenak, J. Faist, and H. Sigg, Nat. Photonics **7**, 466 (2013).
[12]M. Bauer, C. Ritter, P. A. Crozier, J. Ren, J. Menendez, G. Wolf, and J. Kouvetakis, Appl. Phys. Lett. **83**, 2163 (2003).
[13]F. Gencarelli, B. Vincent, L. Souriau, O. Richard, W. Vandervorst, R. Loo, M. Caymax, and M. Heyns, Thin Solid Films **520**, 3211 (2012).

[14]S. Wirths, A. T. Tiedemann, Z. Ikonic, P. Harrison, B. Holländer, T. Stoica, G. Mussler, M. Myronov, D. Buca, and S. Mantl, Appl. Phys. Lett. **102**, 192103 (2013).
[15]S. Wirths, D. Buca, A. T. Tiedemann, P. Bernardy, B. Holländer, T. Stoica, G. Mussler, U. Breuer, and S. Mantl, Solid-State Electron. **83**, 2 (2013).
[16]S. Wirths, D. Buca, G. Mussler, A. T. Tiedemann, B. Holländer, P. Bernardy, T. Stoica, D. Grützmacher, and S. Mantl, ECS J. Solid State Sci. Technol. **2**, N99 (2013).
[17]S. Wirths, D. Buca, A. T. Tiedemann, B. Holländer, P. Bernardy, T. Stoica, D. Grützmacher, and S. Mantl, ECS Trans. **50**(9), 885–893 (2012).
[18]J. M. Hartmann, A. Abbadie, N. Cherkashin, H. Grampeix, and L. Clavelier, Semicond. Sci. Technol. **24**, 055002 (2009).
[19]J. M. Hartmann, J. Appl. Phys. **95**, 5905 (2004).
[20]R. T. Beeler, C. Xu, D. J. Smith, G. Grzybowski, J. Menéndez, and J. Kouvetakis, Appl. Phys. Lett. **101**, 221111 (2012).
[21]G.-E. Chang, S. Chang, and S. L. Chuang, IEEE J. Quantum Electron. **46**, 1813 (2010).
[22]M. Jaros, Phys. Rev. B **37**, 7112 (1988).
[23]H. Trinkaus, D. Buca, B. Holländer, R. A. Minamisawa, S. Mantl, and J. M. Hartmann, J. Appl. Phys. **107**, 124906 (2010).
[24]R. Kotlyar, U. E. Avci, S. Cea, R. Rios, T. D. Linton, K. J. Kuhn, and I. A. Young, Appl. Phys. Lett. **102**, 113106 (2013).
[25]S. Gupta, R. Chen, Y. Huang, Y. Kim, E. Sanchez, J. S. Harris, and K. C. Saraswat, Nano Lett. **13**, 3783 (2013).
[26]G. Sun, R. A. Soref, and H. H. Cheng, J. Appl. Phys. **108**, 033107 (2010).
[27]S. Chang and S. L. Chuang, IEEE J. Quantum Electron. **43**, 249 (2007).
[28]B. Dutt, H. Lin, D. S. Sukhdeo, B. M. Vulovic, S. Gupta, D. Nam, K. C. Saraswat, and J. S. Harris, Jr., IEEE J. Sel. Top. Quantum Electron. **19**, 1502706 (2013).
[29]M. Virgilio, C. L. Manganelli, G. Grosso, G. Pizzi, and G. Capellini, Phys. Rev. B **87**, 235313 (2013).
[30]T. Bahder, Phys. Rev. B **41**, 11992 (1990).
[31]T. Bahder, Phys. Rev. B **46**, 9913 (1992).
[32]K. Lu Low, Y. Yang, G. Han, W. Fan, and Y. Yeo, J. Appl. Phys. **112**, 103715 (2012).
[33]J. Taylor and V. Tolstikhin, J. Appl. Phys. **87**, 1054 (2000).
[34]Y.-F. Lao and A. G. Unil Perera, J. Appl. Phys. **109**, 103528 (2011).